

## Supporting Information

### Pressure-induced remarkable emission enhancement based on intermolecular charge transfer in halogen bond-driven dual-component co-crystals

Aisen Li,<sup>1,2</sup> Jing Wang,<sup>1</sup> Yingjie Liu,<sup>1</sup> Shuping Xu,<sup>1</sup> Ning Chu,<sup>1</sup> Yijia Geng,<sup>1</sup> Bao Li,<sup>1</sup> Bin Xu,<sup>1</sup> Haining Cui,<sup>2\*</sup> and Weiqing Xu<sup>1\*</sup>

1. State Key Laboratory of Supramolecular Structure and Materials, Institute of Theoretical Chemistry, Jilin University, Changchun, 130012, P. R. China

2. College of Physics, Jilin University, Changchun 130012, P. R. China

\*Email: [xuwq@jlu.edu.cn](mailto:xuwq@jlu.edu.cn)  
[cuihn@jlu.edu.cn](mailto:cuihn@jlu.edu.cn)

## Content

1. Raman spectra of pure BIPY and co-crystals.....	2
2. IR spectra of pure BIPY and co-crystals.....	2
3. Single crystal data.....	5
4. Analysis of intermolecular interactions of co-crystals.....	6
5. Hirshfeld surface analysis of co-crystals.....	8
6. Fluorescent spectra of BIPY-IPFB under UV irradiation.....	9
7. Fluorescent spectra properties of BIPY-IFB.....	10
8. The calculated results of BIPY-DITFB.....	11
9. Raman spectra of co-crystals under high pressure.....	12
References.....	14

## 1. Raman spectra of pure BIPY and co-crystals.

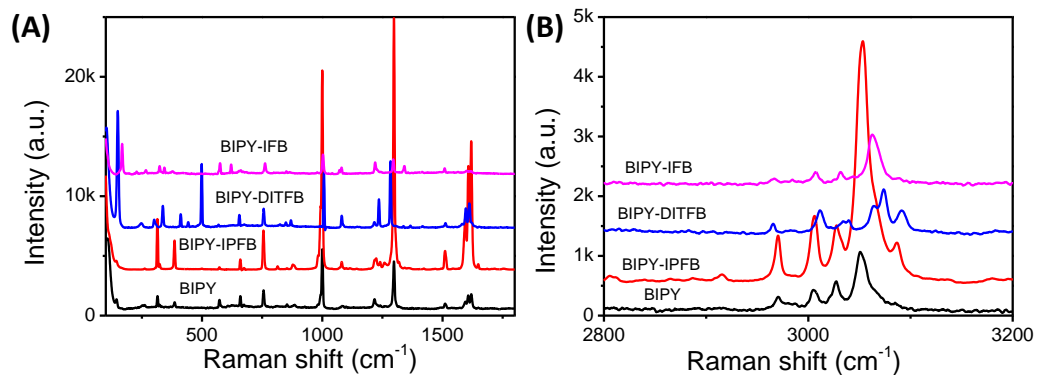


Figure S1. The Raman spectra of BIPY, BIPY-IPFB, BIPY-DITFB, and BIPY-IFB in the ranges of 100-1800 cm<sup>-1</sup> (A) and 2800-3200 cm<sup>-1</sup> (B), respectively.

## 2. IR spectra of pure BIPY and co-crystals.

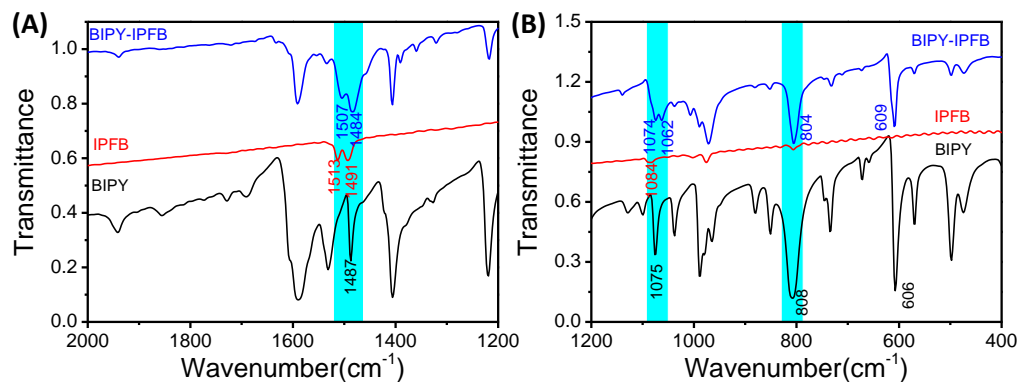


Figure S2. The IR spectra of BIPY (black line), IPFB (red line) and co-crystal BIPY-IPFB (blue line) in the ranges of 1200-2000 cm<sup>-1</sup> (A) and 400-1200 cm<sup>-1</sup> (B), respectively.

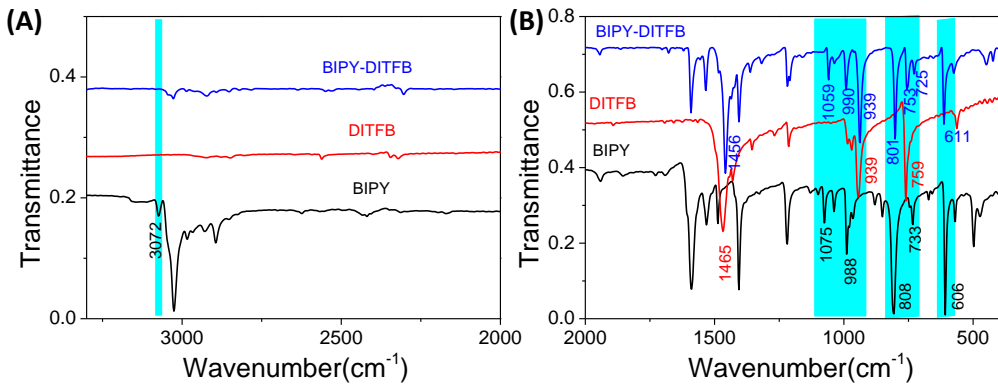


Figure S3. The IR spectra comparison of BIPY (black line), DITFB (red line) and co-crystal BIPY-DITFB (blue line) of  $2000\text{ cm}^{-1}$ - $3600\text{ cm}^{-1}$  (A) and  $400\text{ cm}^{-1}$ - $2000\text{ cm}^{-1}$  (B).

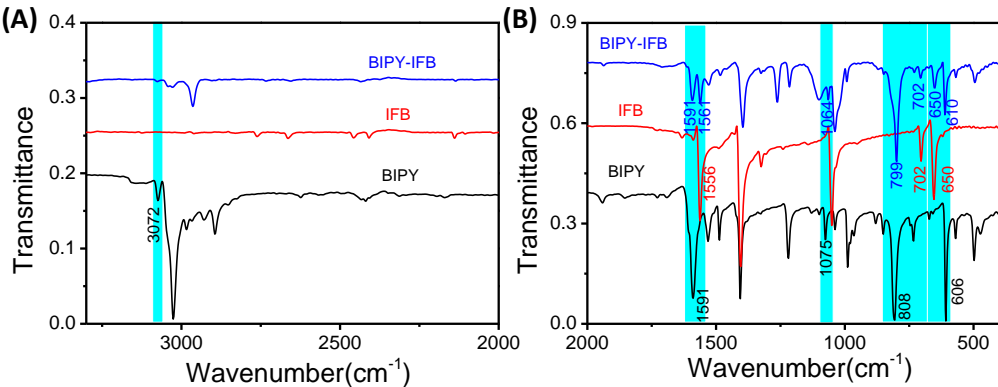


Figure S4. The IR spectra comparison of BIPY (black line), IFB (red line) and co-crystal BIPY-IFB (blue line) of  $2000\text{ cm}^{-1}$ - $3600\text{ cm}^{-1}$  (A) and  $400\text{ cm}^{-1}$ - $2000\text{ cm}^{-1}$  (B).

As displayed in Figure S2, for the pristine BIPY, the characteristic ring breathing vibration bands of pyridine group appear at  $1075\text{ cm}^{-1}$  and  $1487\text{ cm}^{-1}$ , and the peak located at  $606\text{ cm}^{-1}$  and  $808\text{ cm}^{-1}$  can be assigned to ring bending vibration and C-H out-of-plane bending vibration, respectively. And upon assembly with the co-former IPFB, the vibration bands experienced an obvious shift and were located at  $1062\text{ cm}^{-1}$  ( $\Delta = 13\text{ cm}^{-1}$ ),  $1484\text{ cm}^{-1}$  ( $\Delta = 3\text{ cm}^{-1}$ ),  $609\text{ cm}^{-1}$  ( $\Delta = 3\text{ cm}^{-1}$ ) and  $804\text{ cm}^{-1}$  ( $\Delta = 4\text{ cm}^{-1}$ ). At the same time, C-F stretching vibration at  $1084\text{ cm}^{-1}$  of IPFB shifted towards to  $1074\text{ cm}^{-1}$  in BIPY-IPFB, while the bands at  $1491\text{ cm}^{-1}$  and  $1513\text{ cm}^{-1}$  assigned to ring stretching vibration shifted to  $1484\text{ cm}^{-1}$  and  $1507\text{ cm}^{-1}$ . Similarly, in Figure S3, the bands at  $606\text{ cm}^{-1}$ ,  $808\text{ cm}^{-1}$  and  $1075\text{ cm}^{-1}$  also showed obvious

change to  $611\text{ cm}^{-1}$  ( $\Delta = 5\text{ cm}^{-1}$ ),  $801\text{ cm}^{-1}$  ( $\Delta = 7\text{ cm}^{-1}$ ) and  $1056\text{ cm}^{-1}$  ( $\Delta = 19\text{ cm}^{-1}$ ) upon assembly with DITFB. Besides, the C-H out-of-plane bending vibration at  $733\text{ cm}^{-1}$  shifted towards to  $725\text{ cm}^{-1}$ , and the C-H out-of-plane bending vibration at  $3072\text{ cm}^{-1}$  disappeared. Moreover, the C-F symmetrical deformation vibration of DITFB at  $1465\text{ cm}^{-1}$  appeared in the IR spectra of co-crystals at  $1456\text{ cm}^{-1}$ . As described in Figure S4, the bands at  $606\text{ cm}^{-1}$ ,  $808\text{ cm}^{-1}$  and  $1075\text{ cm}^{-1}$  also showed obvious change to  $610\text{ cm}^{-1}$  ( $\Delta = 4\text{ cm}^{-1}$ ),  $799\text{ cm}^{-1}$  ( $\Delta = 9\text{ cm}^{-1}$ ) and  $1064\text{ cm}^{-1}$  ( $\Delta = 11\text{ cm}^{-1}$ ) upon assembly with IFB. The band at  $3072\text{ cm}^{-1}$  also disappeared and the obvious bands at  $650\text{ cm}^{-1}$  and  $702\text{ cm}^{-1}$  attributed to C-F stretching vibration from IFB can be observed in the BIPY-IFB co-crystal. All the spectroscopic changes described above demonstrate the formation of the relative strong halogen bonding interaction (XB) between the co-former and N atoms in the pyridine group.

### 3. Single crystal data.

Table S1. Crystal data and refinement parameters of BIPY-IPFB, BIPY-DITFB and BIPY-IFB.

	BIPY-IPFB	BIPY-DITFB	BIPY-IFB
Moietiy formula	C6 F5 I, 0.5(C10 H8 N2)	C6 F4 I2, C10 H8 N2	C6 F3 I3, C10 H8 N2
Sum formula	C11 H4 F5 I N	C16 H8 F4 I2 N2	C16 H8 F3 I3 N2
Formula wt	372.05	558.04	665.94
T,K	293 K	293 K	273 K
Space group	P 21/c	P 21/c	P n
A, Å	10.102(2)	8.3599(3)	4.1475(3)
B, Å	7.6653(15)	5.7208(2)	9.1050(6)
C, Å	14.953(3)	17.7679(7)	24.1464(17)
$\alpha$ , deg	90	90	90
$\beta$ , deg	93.24(3)	96.344(1)	91.273(3)
$\gamma$ , deg	90	90	90
Volume, Å <sup>3</sup>	1156.0(4)	844.55(5)	911.62(11)
Z	4	2	2
Density, Mg / m <sup>3</sup>	2.138	2.194	2.426
$\mu(M_0 K \alpha)$ , mm <sup>-1</sup>	2.815	3.764	5.172
R(reflections)	0.0317( 2039)	0.0321( 1777)	0.0768( 2872)
wR2(reflections)	0.0702( 2637)	0.0791( 2096)	0.1929( 2887)
Goodness of fit	0.998	0.998	
CCDC	1869982	1869981	1869998

#### 4. Analysis of intermolecular interactions of co-crystals.

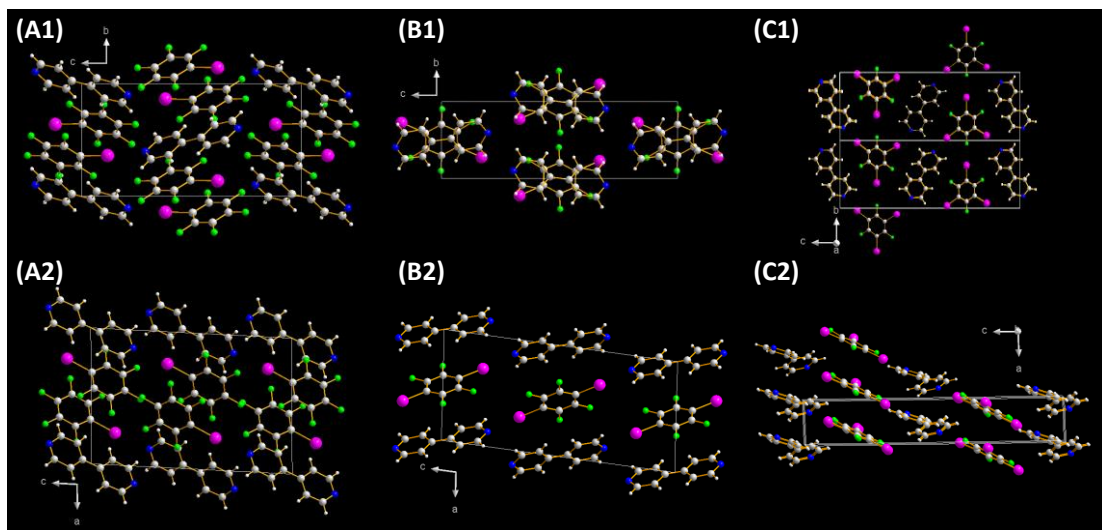


Figure S5. The molecular stacking mode of BIPY-IPFB (A), BIPY-DITFB (B) and BIPY-IFB (C) along **a** axis (1) and **b** axis (2).

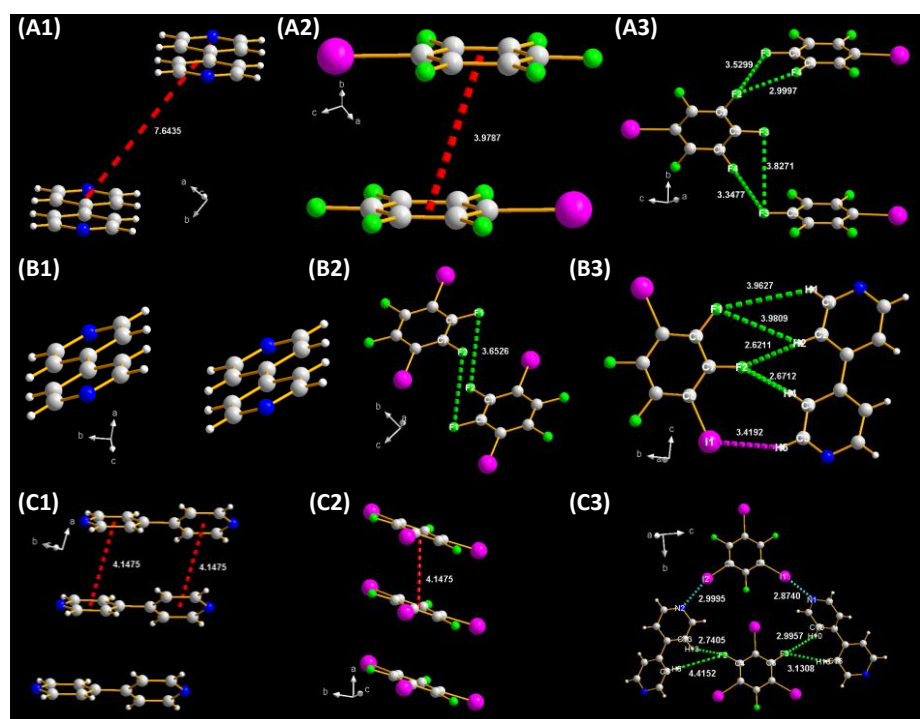


Figure S6. The analysis of intermolecular interactions of BIPY-IPFB (A), BIPY-DITFB (B) and BIPY-IFB (C).

Table S2. The analysis of intermolecular interactions of BIPY-DITFB.

<b>Donor</b>	<b>Hydrogen</b>	<b>Acceptor</b>	<b>DH(Å)</b>	<b>HA(Å)</b>	<b>DA(Å)</b>	<b>DHA(deg)</b>
C2	H2	F2	0.9302	2.6211	3.5269	164
C4	H4	F2	0.9294	2.6712	3.5846	167
C1	H1	F1	0.9302	3.9627	4.6668	135
C2	H2	F1	0.9302	3.9809	4.6661	133
C5	H5	I1	0.9303	3.4192	4.1840	141

Table S3. The analysis of intermolecular interactions of BIPY-IFB.

<b>Donor</b>	<b>Hydrogen</b>	<b>Acceptor</b>	<b>DH(Å)</b>	<b>HA(Å)</b>	<b>DA(Å)</b>	<b>DHA(deg)</b>
C8	H8	F2	0.9298	4.4152	4.9310	118.801
C13	H13	F2	0.9305	2.7405	3.4109	129.701
C10	H10	F3	0.9312	2.9957	3.3434	103.866
C16	H16	F3	0.9307	3.1308	4.0168	159.709
C5	I3	F1	2.0939	3.1000	5.0668	154.102

Firstly, they show different stacking modes because of the difference in co-formers (Figure S5). It should be noted that the BIPY in BIPY-IPFB and BIPY-DITFB show excellent planarity, while it does not for BIPY-IFB, which results from different microenvironments in crystal aggregate state. Moreover, all the co-crystals show parallel stacking and the expected  $\pi\ldots\pi$  interactions are observed for BIPY-IPFB and BIPY-IFB with the distance between the conjugated ring centroids from 3.98 Å to 4.15 Å, respectively (Figure S6A2, S6C1 and S6C2). Additionally, the CH...F hydrogen bonds can be observed between the BIPY and fluorine-containing units in the BIPY-DITFB and BIPY-IFB co-crystals (Figure S6B3, S6C3) and the detailed measurements are summarized in Table S2 and Table S3. As illustrated in Figure S6C3, a zig-zag halogen-bonding chain is produced for BIPY-IFB and connected with the adjacent one by I...F close contacts ( $dI\cdots F = 3.1000$  Å in Table S3). And the C-F...F-C weak noncovalent interactions are also shown in Figure S6A3 and S6B2 for BIPY-IPFB and BIPY-DITFB, which are known to be stabilizing and give significant energy contributions for structures, as Pauling's principle states that the

attractive interatomic dispersion forces would be low because of the low polarizability of fluorine.<sup>1,2</sup> Therefore, the introduction of electron withdrawing substituents (such as -F) on the co-formers affords 3D architectures due to their ability to simultaneously participate in additional intermolecular interactions besides the enhanced I...N interactions.

## 5. Hirshfeld surface analysis of co-crystals.

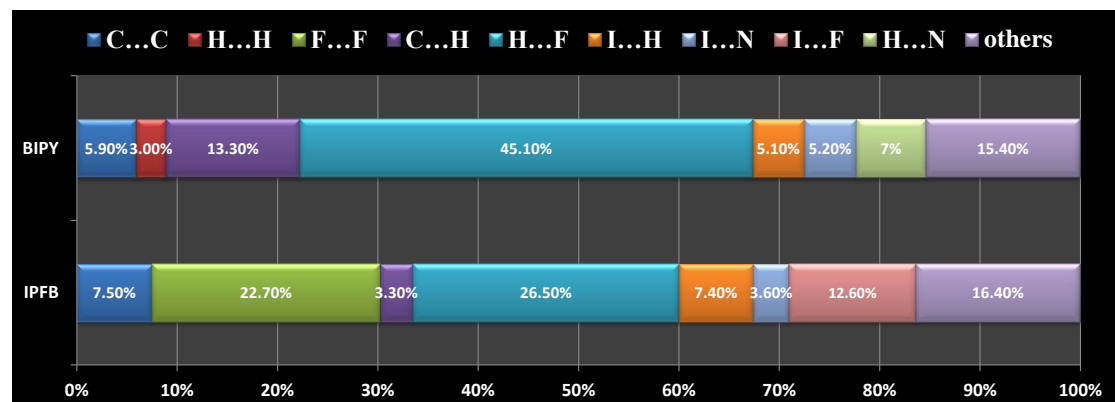


Figure S7. Distribution of individual intermolecular interactions of each part in BIPY-IPFB co-crystal of on the basis of Hirshfeld surface analysis.

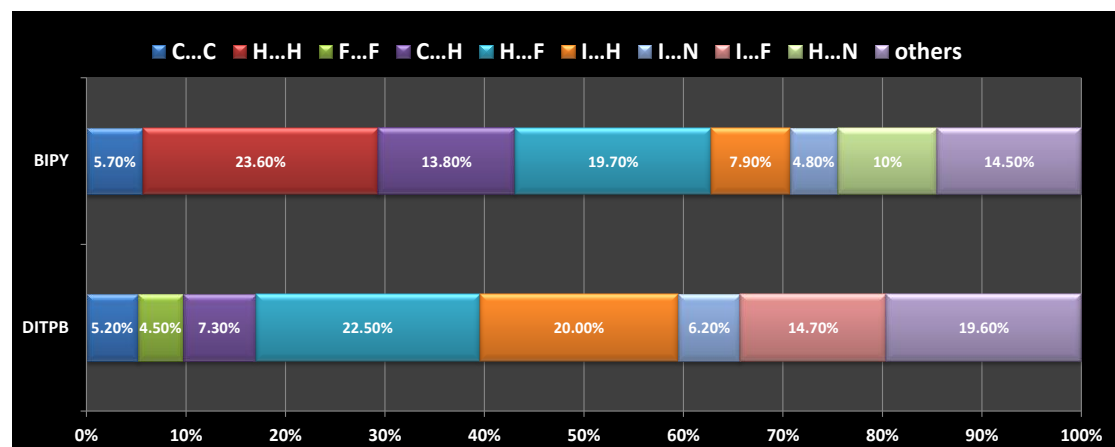


Figure S8. Distribution of individual intermolecular interactions of each part in BIPY-DITFB co-crystal of on the basis of Hirshfeld surface analysis.

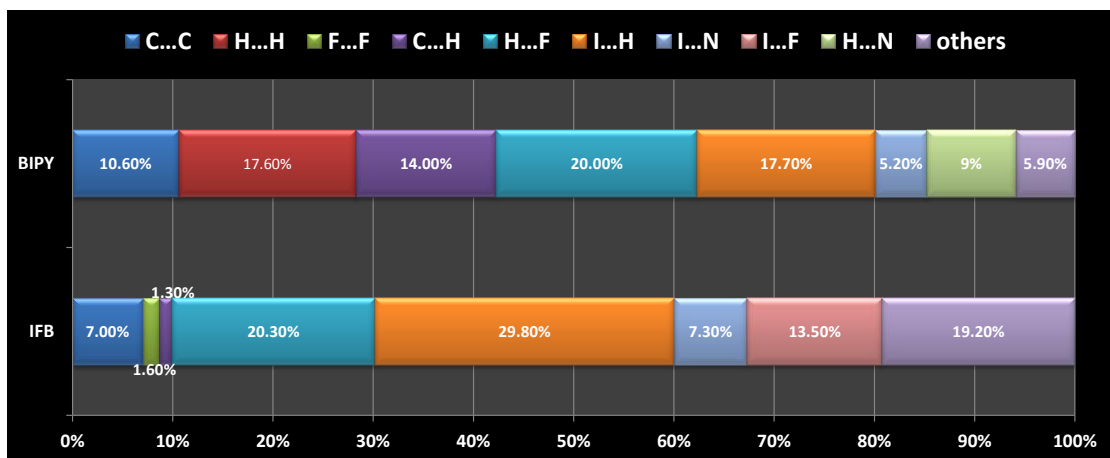


Figure S9. Distribution of individual intermolecular interactions of each part in BIPY-IFB co-crystal of on the basis of Hirshfeld surface analysis.

## 6. Fluorescent spectra of BIPY-IPFB under UV irradiation.

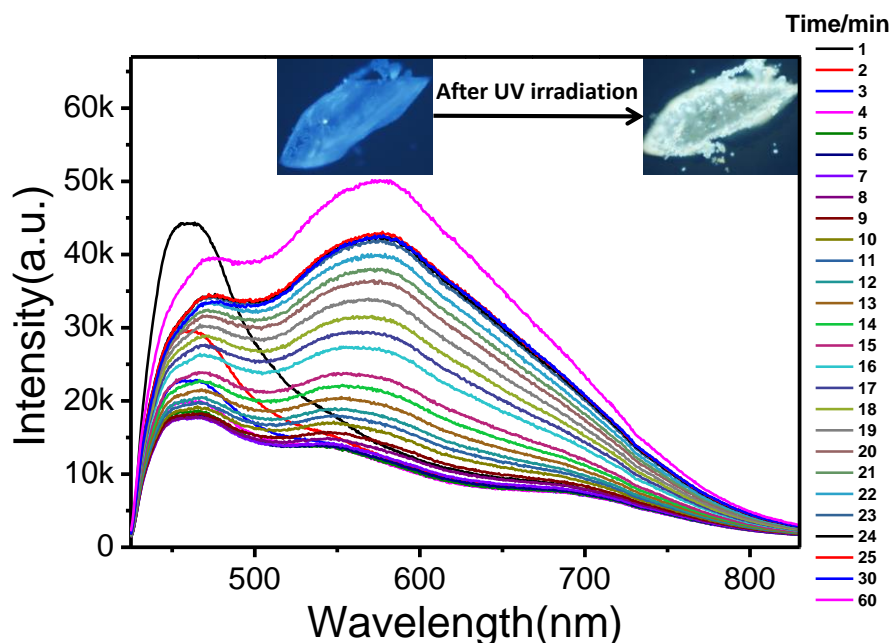


Figure S10. The variation of *in situ* fluorescent spectra of BIPY-IPFB after UV irradiation as UV irradiation time increasing.

## 7. Fluorescent spectra properties of BIPY-IFB.

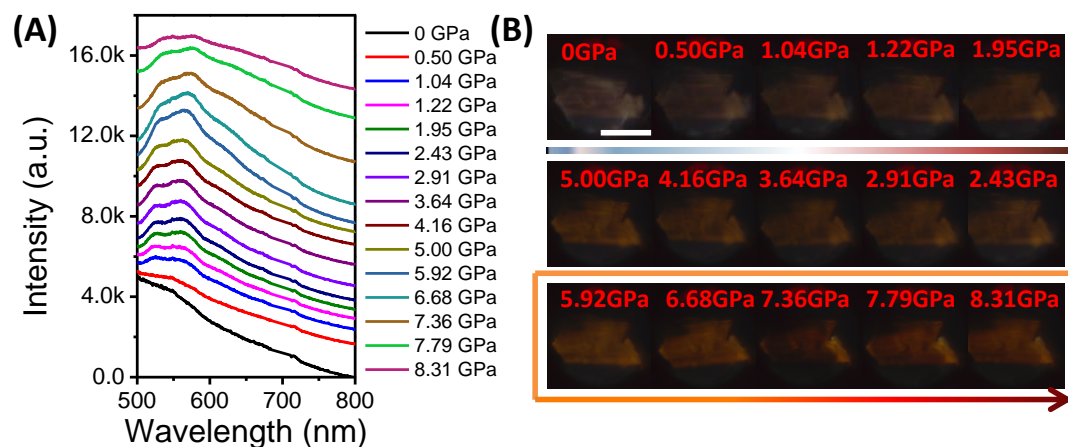


Figure S11. (A) The fluorescent spectra of BIPY-IFB co-crystal during compression and corresponding photos (B) *via* DAC device. Excitation wavelength was 365 nm. The scale is 100  $\mu$ m.

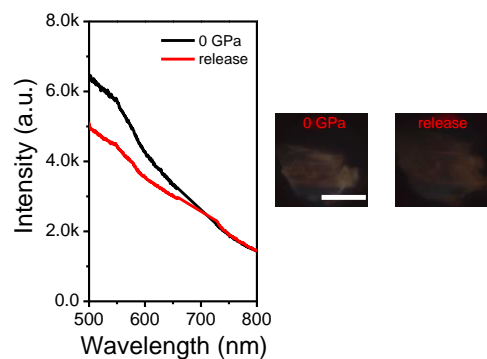


Figure S12. The fluorescent spectra recovery properties of BIPY-IFB co-crystal *via* DAC. Excitation wavelength was 365 nm.

## 8. The calculated results of BIPY-DITFB.

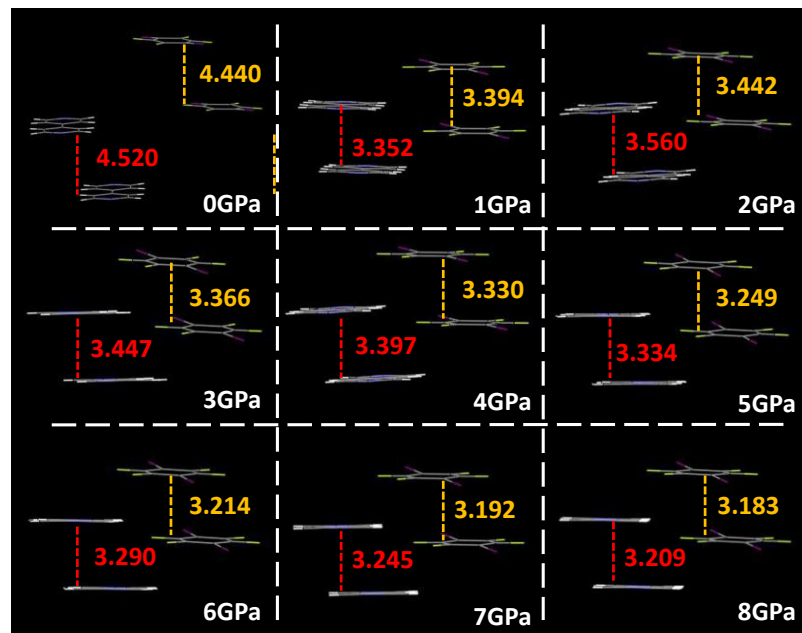


Figure S13. Calculated stacking structure of BIPY-DITFB under different pressure and the detailed measurement of distances between adjacent BIPY molecules or DITFB molecules for comparison.

## 9. Raman spectra of co-crystals under high pressure.

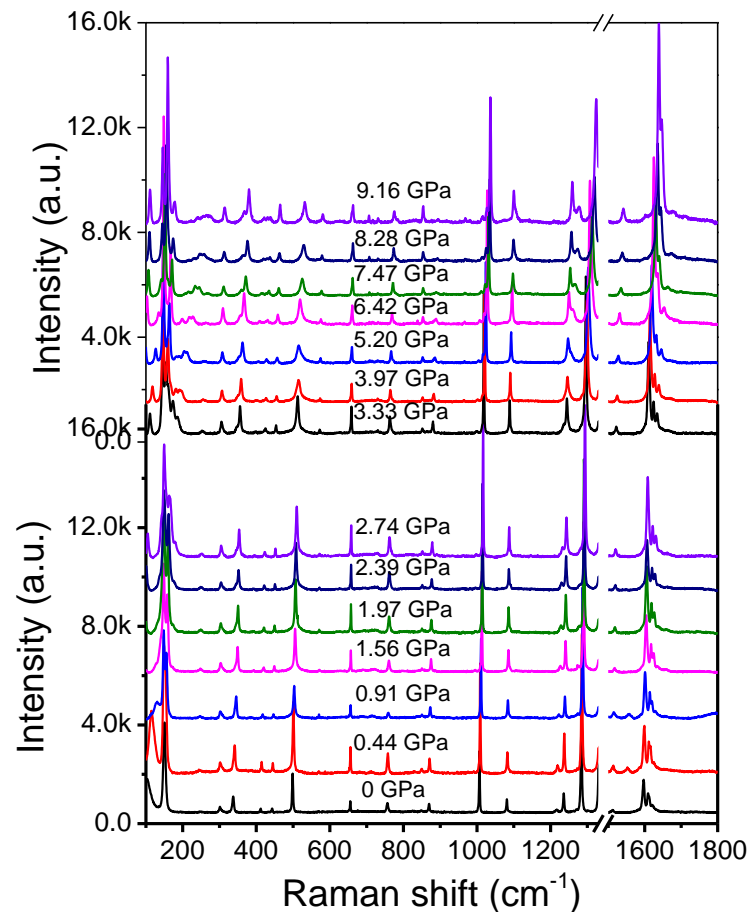


Figure S14. Raman spectra of BIPY-DITFB co-crystal at different pressure values via DAC up to 9.16 GPa. Excitation wavelength was 633 nm.

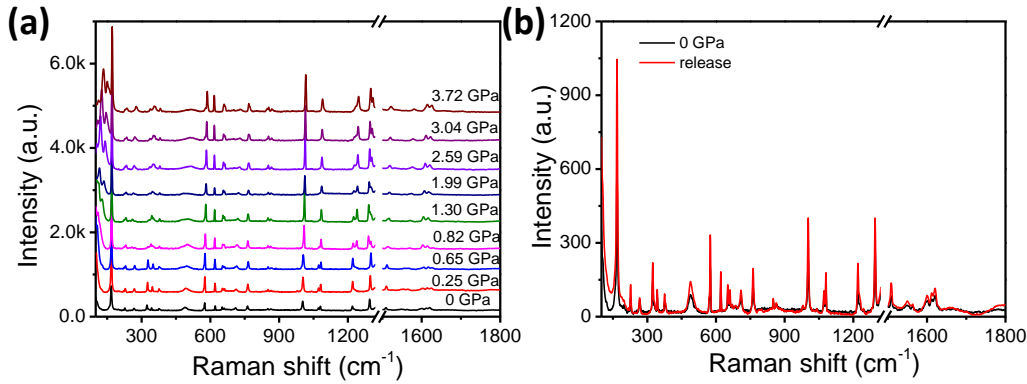


Figure S15. (a) Raman spectra of BIPY-IFB co-crystal at different pressure values via DAC up to 3.72 Gpa, and the recovered Raman spectra of the BIPY-IFB co-crystal after the decompression. Excitation wavelength was 633 nm.

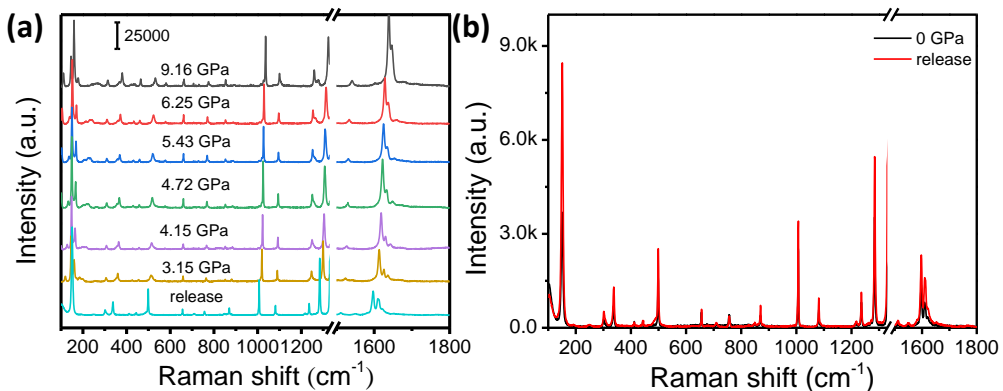


Figure S16. Raman spectra of the BIPY-DITBF co-crystal upon the decompression process (a) and the recovery of the BIPY-DITBF (b). Excitation wavelength was 633 nm.

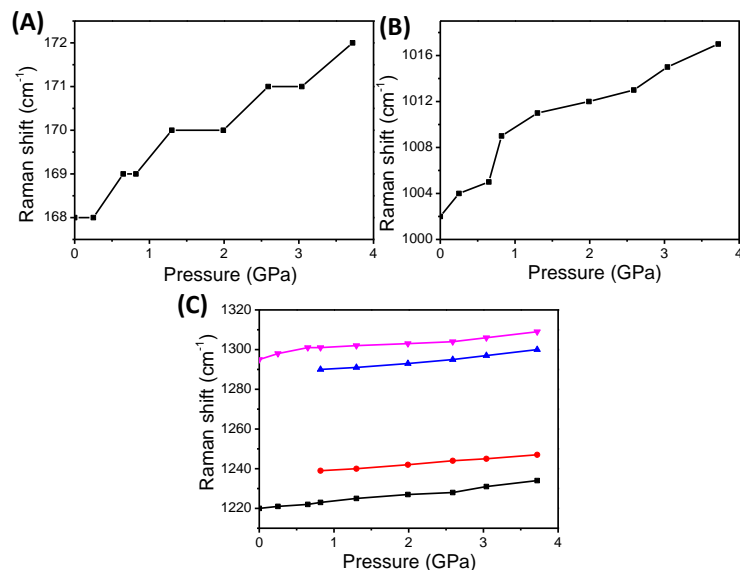


Figure S17. Pressure dependence of Raman shifts  $168 \text{ cm}^{-1}$  (A),  $1002 \text{ cm}^{-1}$  (B),  $1220, 1239, 1295$  and  $1301 \text{ cm}^{-1}$  (C) in BIPY-IFB co-crystal.

Table S4. Assignment and frequencies ( $\text{cm}^{-1}$ ) of observed Raman internal modes of BIPY-DITFB co-crystal in comparison with DFT simulation results.

<b>Experimental value (<math>\text{cm}^{-1}</math>)</b>	<b>Theoretical value (<math>\text{cm}^{-1}</math>)</b>	<b>Vibrational mode</b>
150	149	C-I stretching vibration
1007	1009	Triangular ring breathing vibration of BIPY
1216	1235	C-H rocking vibration in plane
1236	1240	C-H rocking vibration in plane ring breathing vibration of DITFB
1284	1305	C-C stretching vibration ring breathing vibration of BIPY C-H rocking vibration in plane
1597	1621	C=C=C antisymmetric stretching vibration of DITFB
1609	1628	C=C=C antisymmetric stretching vibration of BIPY C-C stretching vibration
1612	1637	C=C=C antisymmetric stretching vibration of BIPY C-C stretching vibration

Table S5. Assignment and frequencies ( $\text{cm}^{-1}$ ) of observed Raman internal modes of BIPY-IFB co-crystal in comparison with DFT simulation results.

<b>Experimental value (<math>\text{cm}^{-1}</math>)</b>	<b>Theoretical value (<math>\text{cm}^{-1}</math>)</b>	<b>Vibrational mode</b>
168	165	C-I stretching vibration
1002	1003	Triangular ring breathing vibration of BIPY
1220	1238	C-H rocking vibration in plane
1295	1305	C=C=C antisymmetric stretching vibration of IFB C-H rocking vibration in plane C-C stretching vibration

## References

1. V. G. Saraswatula and B. K. Saha, *New J. Chem.*, 2014, **38**, 897-901. .
2. K. Reichenbacher, H. I. Suss and J. Hulliger, *Chem. Soc. Rev.*, 2005, **34**, 22-30.